

Supporting Information

Experimental Demonstration of In-memory Computing using Pressure Stimulated SnO_{2-x} -Based Memristive Device as Inverter and active-low 2:1 Multiplexer

Bishal Kumar Keshari¹, Soumi Saha¹, Sanghamitra DebRoy², Akshay Salimath², Venkat Mattela³, Subhradeep Pal¹, Surya Shankar Dan¹ and Parikshit Sahatiya^{1,*}

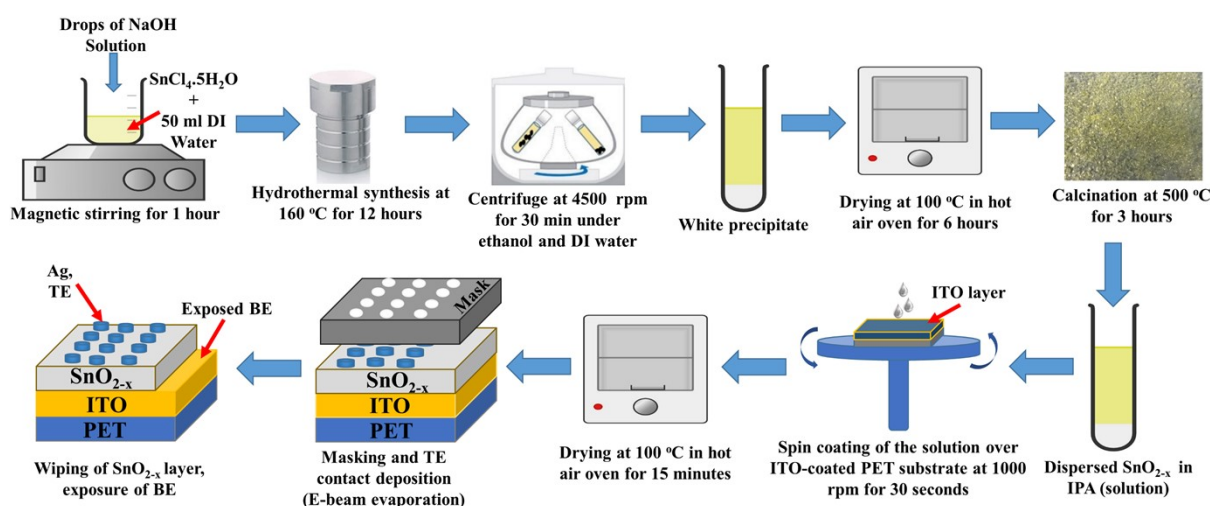


Figure S1. Illustration for the synthesis of SnO_{2-x} and device fabrication of the Ag/ SnO_{2-x} /ITO memristive device.

The Energy Dispersive Spectroscopy (EDS) was performed on the tin oxide layer spin-coated on ITO/PET substrate and identified the elements (i.e. Sn, O) as shown in Figure S2. As per the EDS spectra shown in Figure S2(a), the obtained atomic percentages of oxygen and tin are 65.10 % and 34.90 %, respectively. Under the consideration of stoichiometric tin oxide (SnO_2), the atomic ratio of oxygen to tin should be 2:1, and hence, the expected atomic percentage of the same elements should be around 66.67 % and 33.33 %, respectively. The obtained atomic percentage value of oxygen in the coated tin oxide layer is lower than that of its stoichiometric value (i.e. 66.67 %). This lower atomic percentage of oxygen in the coated tin oxide layer reveals that the hydrothermally synthesized tin oxide material has oxygen deficiency or oxygen vacancy inherently. This supports the claim of the presence of oxygen vacancies in the hydrothermally synthesized tin oxide (SnO_{2-x}) made by the XPS analysis (Figure 1(d) in the manuscript). However, the larger intensity peak of Sn than that of O, as can be observed in Figure S2(a), is due to the fact that tin is heavier than that of oxygen, which has also been

reflected in the color-mapped EDS layered images of the Sn and O elements under the exposed SnO_{2-x} region as shown Figure S2(b-d).¹

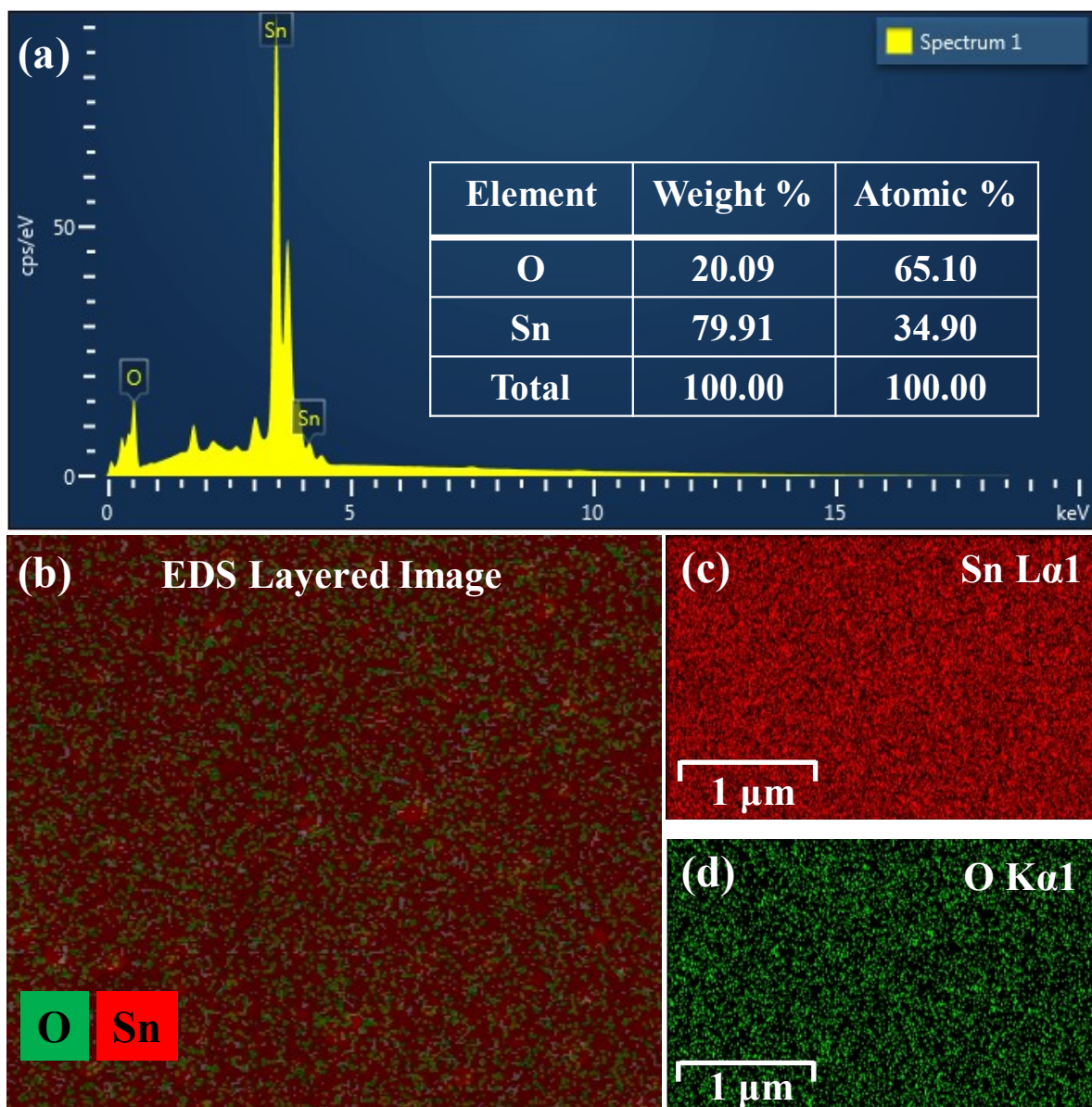


Figure S2. (a) EDS spectra of tin oxide (SnO_{2-x}) film, synthesized by hydrothermal method (b) EDS layered image of Sn and O elements present on SnO_{2-x} spin-coated film (c, d) Elemental mapping of Sn and O elements under the exposed SnO_{2-x} region, respectively.

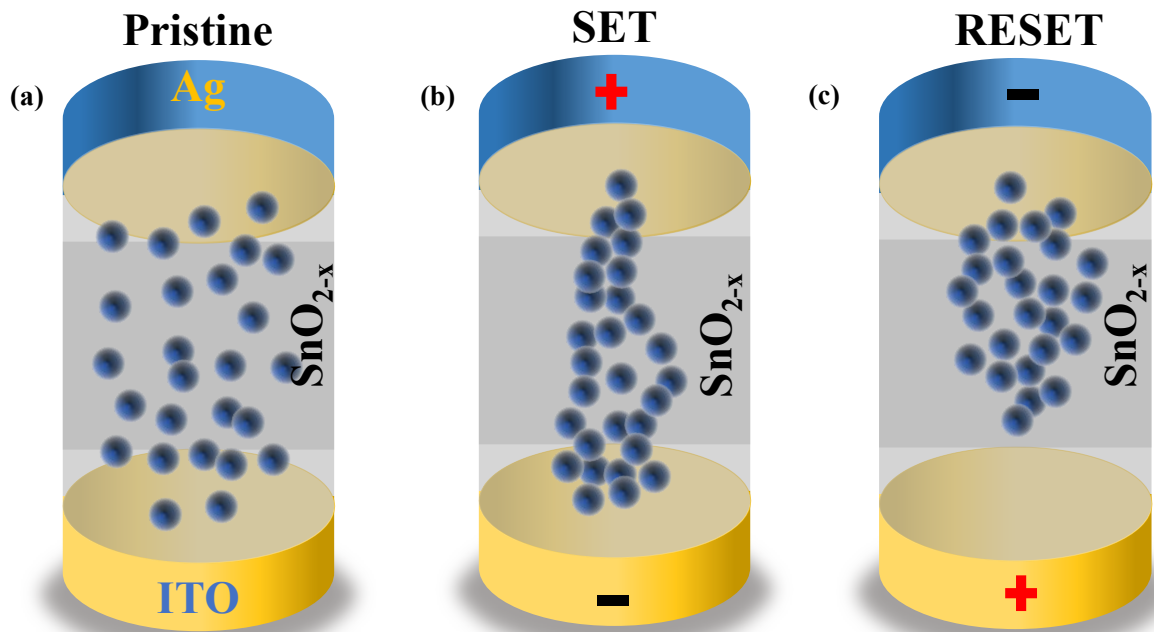


Figure S3. Schematic illustration of oxygen vacancy-based resistive switching mechanism in the fabricated Ag/SnO_{2-x}/ITO memristive device from (a) pristine state to (b) LRS or SET when Ag TE was positively biased to (c) HRS or RESET when Ag TE was negatively biased under the applied voltage sweep.

Oxygen vacancies are positively charged and considered mobile species, which play a significant role in resistive switching in the Valence Change Memory (VCM) type of memristive devices.² As per some empirical studies on metal oxides, it has been reported that oxygen vacancies tend to migrate along the direction of the applied electric field.^{3,4} Therefore, it can be assumed that the oxygen vacancy migration along the direction of the electric field is one of the main features of the fabricated Ag/SnO_{2-x}/ITO memristive device, which plays a vital role in achieving a forming free gradual resistive switching phenomena in the device. However, the gradual SET and RESET phenomena, as observed in the I-V characteristics as shown in Figure 4(b) (in the main article), indicate that the fabricated device is indeed a VCM type of memristive device, and the discussed mechanism has been illustrated in Figure S3.^{5,6} As shown in Figure S3(a), the oxygen vacancies are intrinsically randomly distributed in the pristine SnO_{2-x} layer. The oxygen vacancies arrange themselves along the direction of the applied electric field and form a conductive path between the top and bottom electrodes. Due to this low resistive conductive path formation, the device enters into its LRS, as shown in Figure S3(b). Further, when the applied electric field gets reversed, there could be the dissolution of the conductive path due to the migration of oxygen vacancies in the opposite

direction, and the conductive path is likely to be detached from the ITO BE, as shown in Figure S3(c), this may cause the device to pursue it HRS. In a similar manner, the SET and RESET phenomenon of the fabricated Ag/SnO_{2-x}/ITO memristive device for the subsequent voltage sweep cycles might have taken place.

To test the pulse endurance characteristics of the Ag/SnO_{2-x}/ITO memristive device, a voltage pulse scheme, same for electrical (no pressure) and at different pressure conditions, was applied as shown in Figures S4(a) and S4(b), respectively. The pulse cycle mainly consists of a read voltage pulse of 0.2V, a SET pulse of 2.2V to guarantee the switching of the resistance state to LRS, and a RESET pulse of -2.2V to ensure HRS in the device evident from the recorded current response shown in Figures S4(a) and S4(b), for electrical (no pressure) and at different pressure conditions respectively. The pulse widths of the read, SET, and RESET operations were set to 60 ms, 100 ms, and 100 ms, respectively.

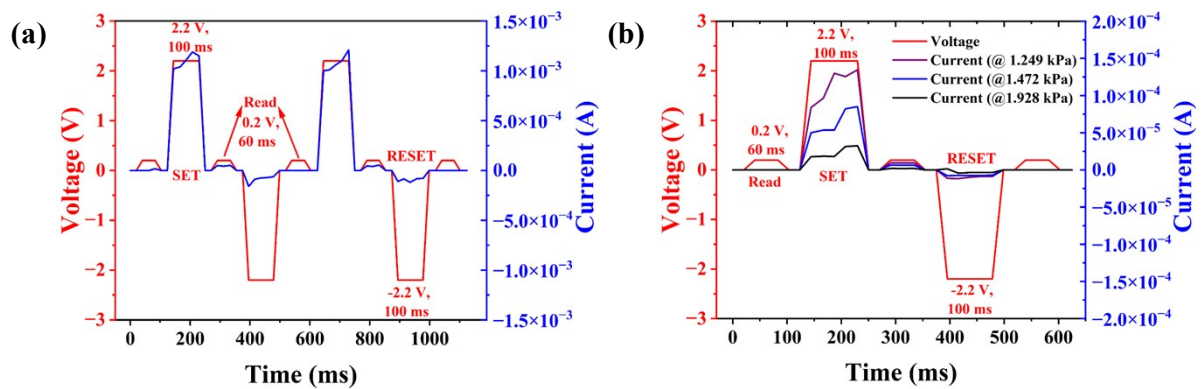


Figure S4. (a) Measured current responses during the applied SET (2.2 V, 100 ms pulse width), RESET (-2.2 V, 100 ms pulse width) and READ (0.2 V, 60 ms pulse width) pulse scheme under no pressure condition. (b) Measured current responses during the applied SET (2.2 V, 100 ms pulse width), RESET (-2.2 V, 100 ms pulse width) and READ (0.2 V, 60 ms pulse width) pulse scheme under 1.249 kPa, 1.472 kPa, and 1.928 kPa pressure conditions.

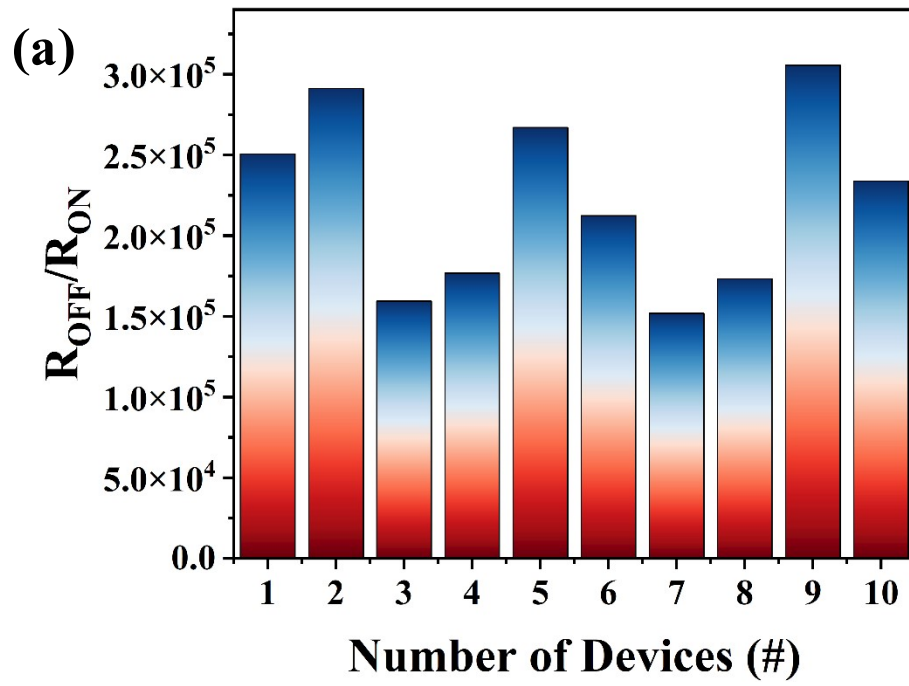


Figure S5. Device-to-device variation of the resistance window (R_{OFF}/R_{ON}) value of ten different devices, showing insignificant variation in the order.

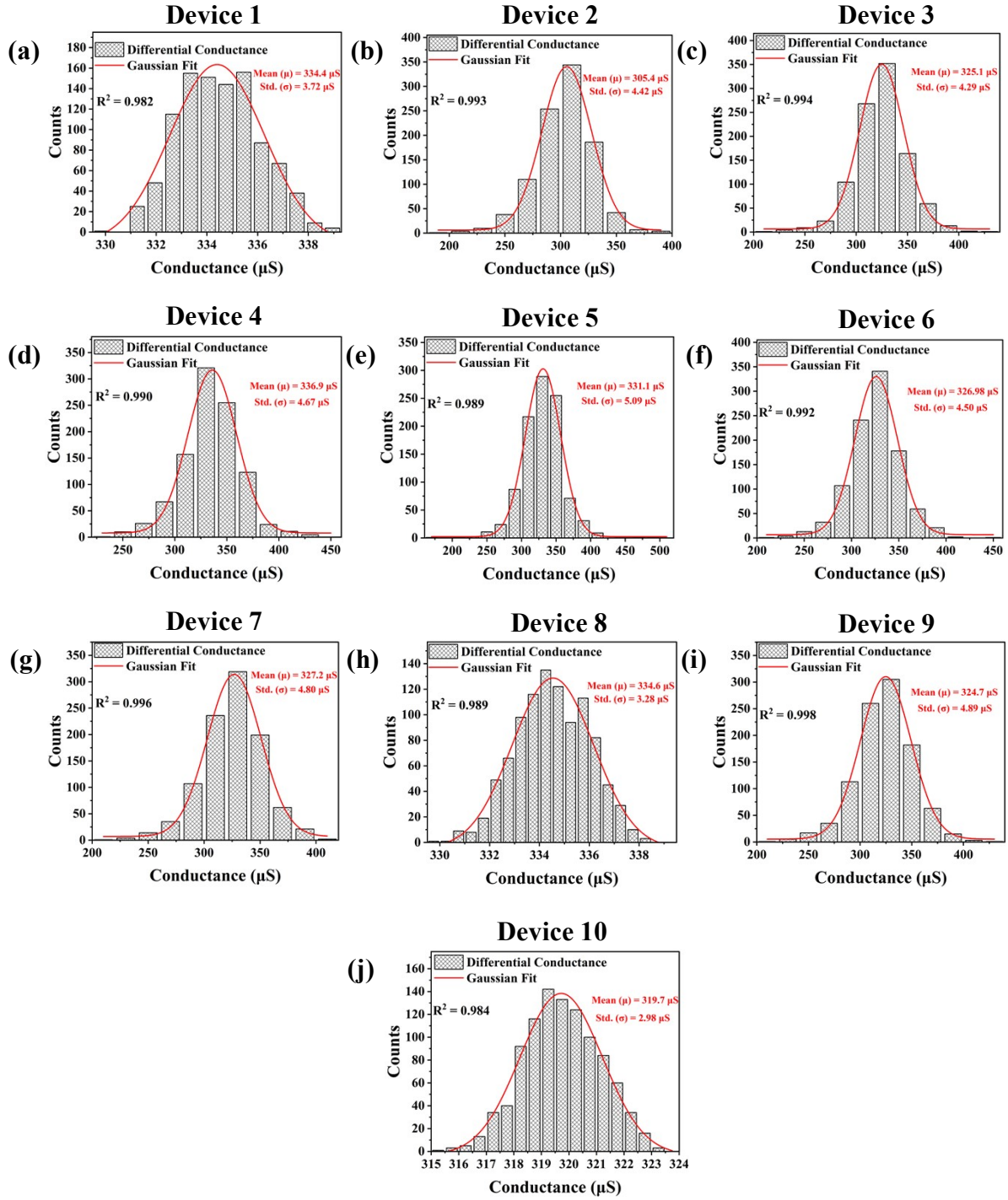


Figure S6. Differential conductance distribution under the LRS for different devices with 1×10^3 switching cycles.

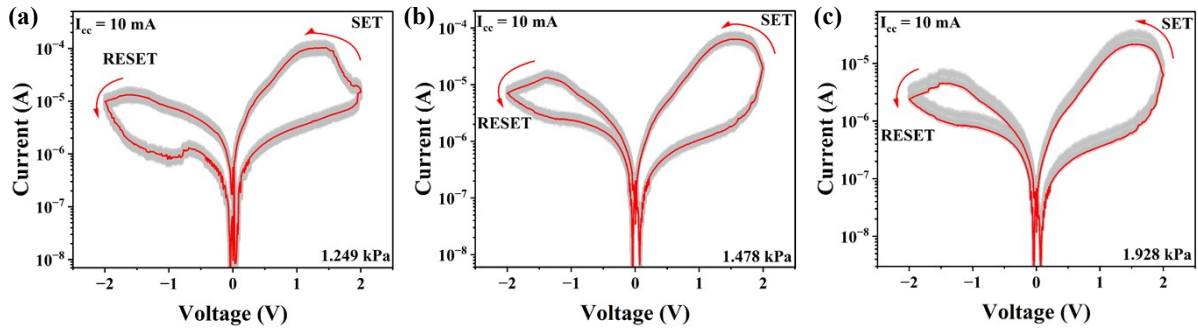


Figure S7. (a) 100-cycle DC IV characteristics of PDMS encapsulated Ag/SnO_{2-x}/ITO memristive device at (a) 1.249 kPa pressure, (b) 1.478 kPa pressure, (c) 1.928 kPa pressure, respectively.

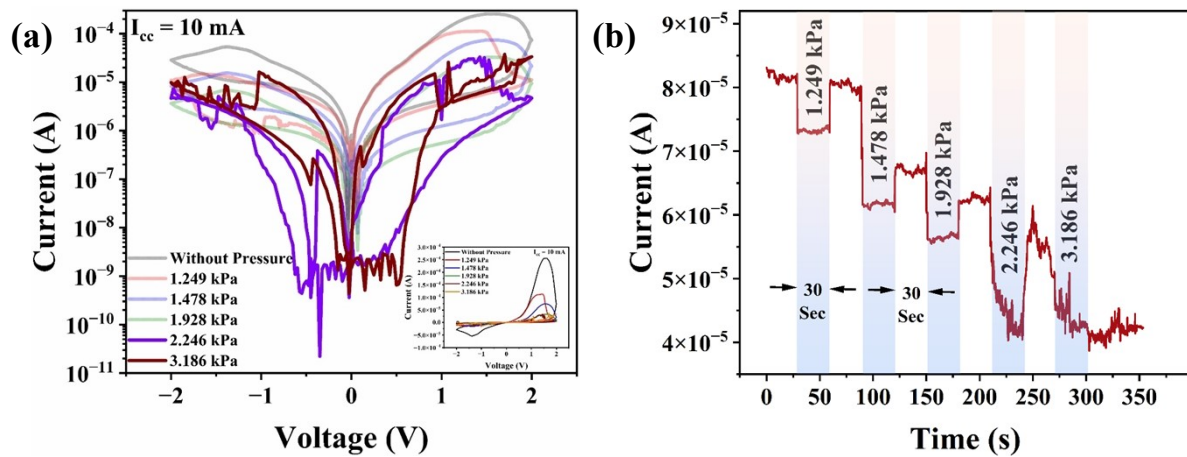


Figure S8. (a) I-V characteristics of the Ag/SnO_{2-x}/ITO device at extended pressure values of 2.24 kPa and 3.186 kPa, respectively, on the semilog scale (inset: linear scale) (b) Temporal response of the device current under different applied pressure amplitudes.

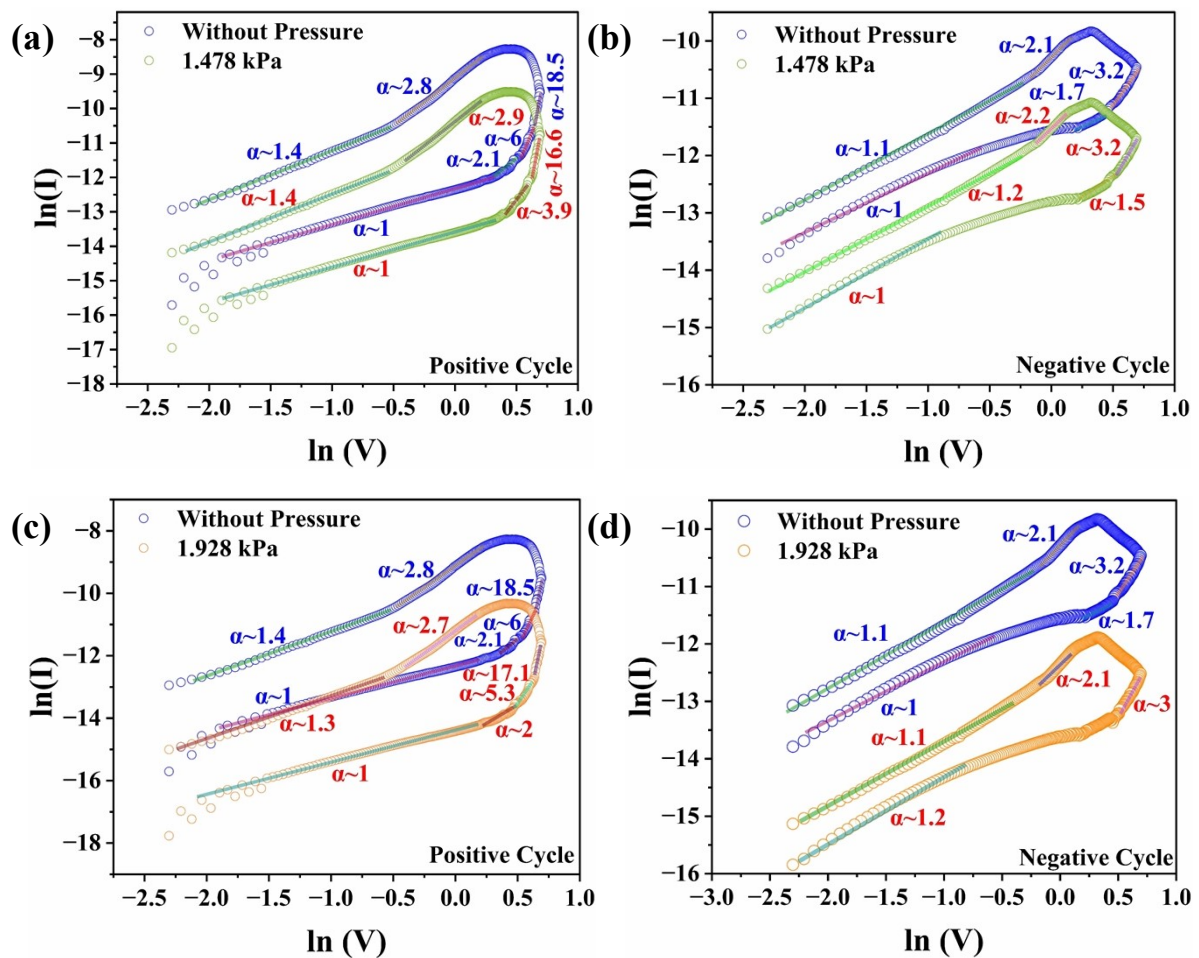


Figure S9. (a) Double-log-fitted positive cycle I-V behavior of Ag/SnO_{2-x}/ITO memristive device under without pressure and 1.478 kPa pressure conditions, (b) Double-log-fitted negative cycle I-V behavior of Ag/SnO_{2-x}/ITO memristive device under without pressure and 1.478 kPa pressure conditions, (c) Double-log-fitted positive cycle I-V behavior of Ag/SnO_{2-x}/ITO memristive device under without pressure and 1.928 kPa pressure conditions, (d) Double-log-fitted negative cycle I-V behavior of Ag/SnO_{2-x}/ITO memristive device under without pressure and 1.928 kPa pressure conditions.

References:

1. Goldstein, J. I. *et al.* *Microscopy and X-Ray Microanalysis*.
2. Yang, J. J., Strukov, D. B. & Stewart, D. R. Memristive devices for computing. *Nat. Nanotechnol.* **8**, 13–24 (2013).
3. Kwon, D. H. *et al.* Atomic structure of conducting nanofilaments in TiO₂ resistive switching memory. *Nat. Nanotechnol.* **5**, 148–153 (2010).
4. Di Martino, G. *et al.* Real-time in situ optical tracking of oxygen vacancy migration in memristors. *Nat. Electron.* **3**, 687–693 (2020).
5. Wong, H. S. P. *et al.* Metal-oxide RRAM. *Proc. IEEE* **100**, 1951–1970 (2012).
6. Mohammad, B. *et al.* State of the art of metal oxide memristor devices. *Nanotechnol. Rev.* **5**, 311–329 (2016).